Growth changes in the anterior and middle cranial bases assessed with cone-beam computed tomography in adolescents

Mona Afrand,[a] Heesoo Oh,[b] Carlos Flores-Mir,[a] and Manuel O. Lagravère-Vich[a]
Edmonton, Alberta, Canada, and San Francisco, Calif

Introduction: Initially, cone-beam computed tomography images from dry skulls were used to 3 dimensionally evaluate intrarater and interrater reliabilities and accuracy of selected 3-dimensional landmarks located in the anterior and middle cranial bases. Thereafter, dimensional changes of the anterior and middle cranial bases with growth were evaluated by using the previously selected landmarks. **Methods:** Cone-beam computed tomography images of 10 dry skulls were used to identify useful landmarks from different areas of the anterior and middle cranial bases based on their reliability and accuracy. These selected landmarks were identified in the images of an already available sample of adolescents (n = 60) taken at 2 time points (19 months apart) to assess dimensional changes with growth. **Results:** The majority of the proposed 3-dimensional landmarks with the exception of the lesser wing of the sphenoid showed acceptable intrarater and interrater reliabilities. The distances measured between foramina and canals in the transverse dimension showed evidence of increases in size. However, the mean amounts of increase in these transverse distances were equal to or less than 1.05 mm (from 1.1% to 4.1%). No change was observed between the right and left anterior and posterior clinoid processes. The vertical dimensions showed evidence of some changes, but these were within 2% of the original distances. **Conclusions:** In this adolescent sample, minor growth-related changes were observed in the anterior and middle cranial bases. The midsagittal area of the anterior cranial base (foramen caecum to presphenoid) was stable. The right and left anterior and posterior clinoid processes can be used for transverse superimposition. (Am J Orthod Dentofacial Orthop 2017;151:342-50)

Craniofacial growth and development knowledge is a cornerstone concept for the orthodontic specialty. Without an understanding of the normal growth pattern of the head, an orthodontist's diagnosis and treatment planning is most likely destined to fail. Studies have stated that the anterior cranial base growth is completed early in life and even significantly before other craniofacial structures.[1,2]

[a]Department of Dentistry, Faculty of Medicine and Dentistry, University of Alberta, Edmonton, Alberta, Canada.
[b]Department of Orthodontics, Arthur A. Dugoni School of Dentistry, University of the Pacific, San Francisco, Calif.
All authors have completed and submitted the ICMJE Form for Disclosure of Potential Conflicts of Interest, and none were reported.
Address correspondence to: Manuel O. Lagravère-Vich, Department of Dentistry, University of Alberta, ECHA 5-524, Edmonton, AB, Canada; e-mail, manuel@ualberta.ca.
Submitted, July 2015; revised and accepted, February 2016.
0889-5406/$36.00

http://dx.doi.org/10.1016/j.ajodo.2016.02.032

About 86% of the growth of the anterior cranial base is considered complete by the age of 4.5 years, and the remaining growth contributes to increases in the length of the anterior cranial base (sella-nasion) even after puberty.[2] This means that the remaining 14% will be completed over a span of 12 to 18 years. Even considering this previous knowledge, the anterior cranial base has been used as a reference structure in diagnosis, treatment planning, and evaluation of treatment outcomes and changes during treatment of the craniofacial complex.

An analysis of the expected normal growth changes in the anterior cranial base is important. Increases in the thickness of the frontal bone, apposition in the glabella region, and the size of the frontal sinus contribute to increases in the length of the anterior cranial base for measurements such as the sella-nasion line due to the forward movement of nasion until adulthood (3.3% increase in this area of the frontal bone segment from age 6 to early adulthood[3]).[1,4,5] The anteroposterior length of the presphenoid region was reported to be stable after the

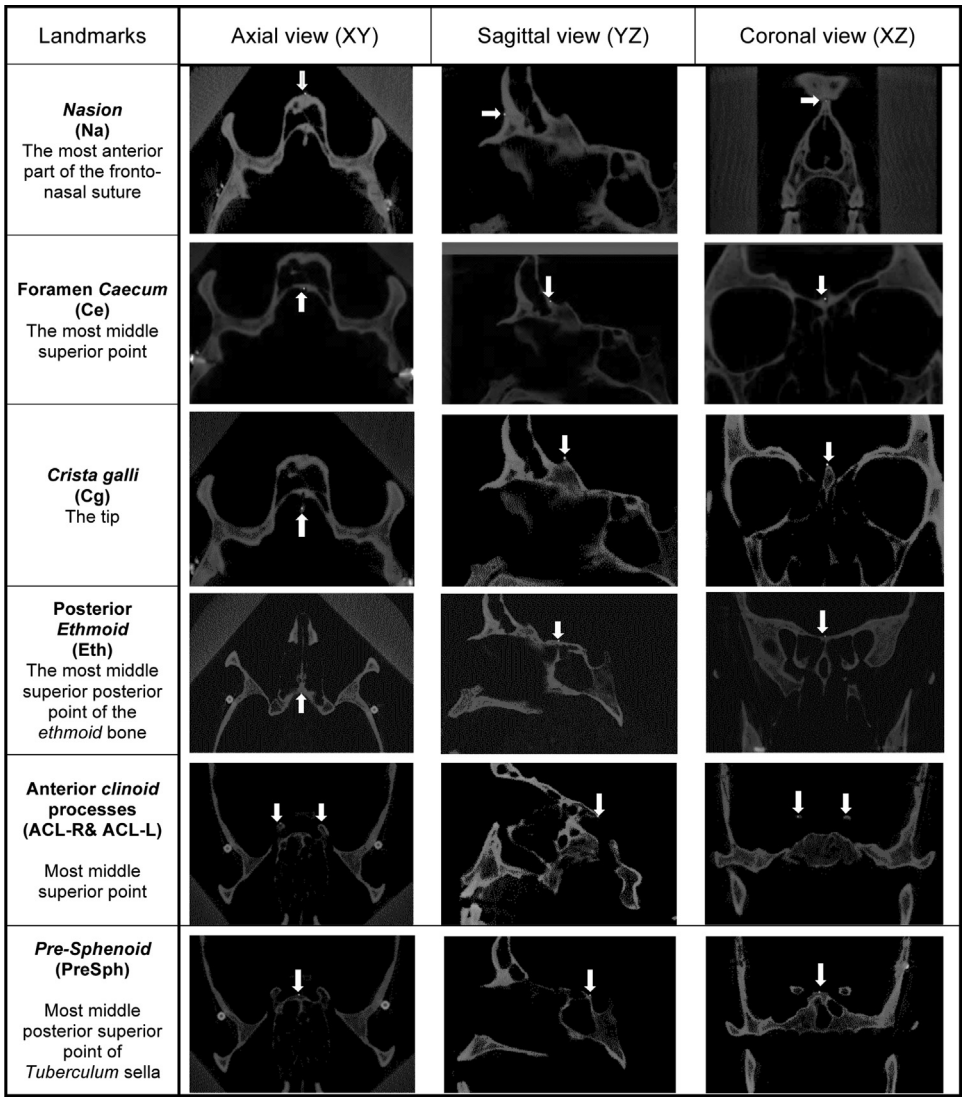

Fig. Three-dimensional landmarks on CBCT images of a dry skull.

age of 7 years as assessed by cross-sectional and longitudinal studies.[1,3,6] Björk[4] observed remodeling of sella turcica during growth, resulting in displacement of sella downward and backward. He recorded an elevation of the tuberculum sella in relation to other structures of the anterior cranial fossa. The cribriform plate of the ethmoid is also considered stable after the age of 4 years.[1,3]

As one can observe, changes in the anterior cranial fossa during postnatal growth are predominantly sagittal growth changes. To determine the stability of structures in all 3 planes of space (anteroposterior, transverse, and vertical), further analysis of the other planes is required.[7]

Nowadays, for dental and maxillofacial surgery and orthodontic applications, cone-beam computed tomography (CBCT) can potentially overcome some limitations of all other previous imaging methods and measuring techniques. Analysis of CBCT images allows assessment of 3-dimensional (3D) dental, skeletal, and soft-tissue changes for both growing and nongrowing patients.

Based on this introduction, 3D changes in size and displacement of the cranial base structures outside the sagittal plane have not been synthesized in detail yet. In our study, the anterior and middle cranial base structural changes due to growth in adolescents were assessed in 3 dimensions using CBCT. Therefore, this article has 2 parts. First, intrarater and interrater reliabilities of selected landmarks in the anterior cranial base were assessed; second, the changes in the linear measurements derived from the proposed and validated landmarks were evaluated between 2 time points.

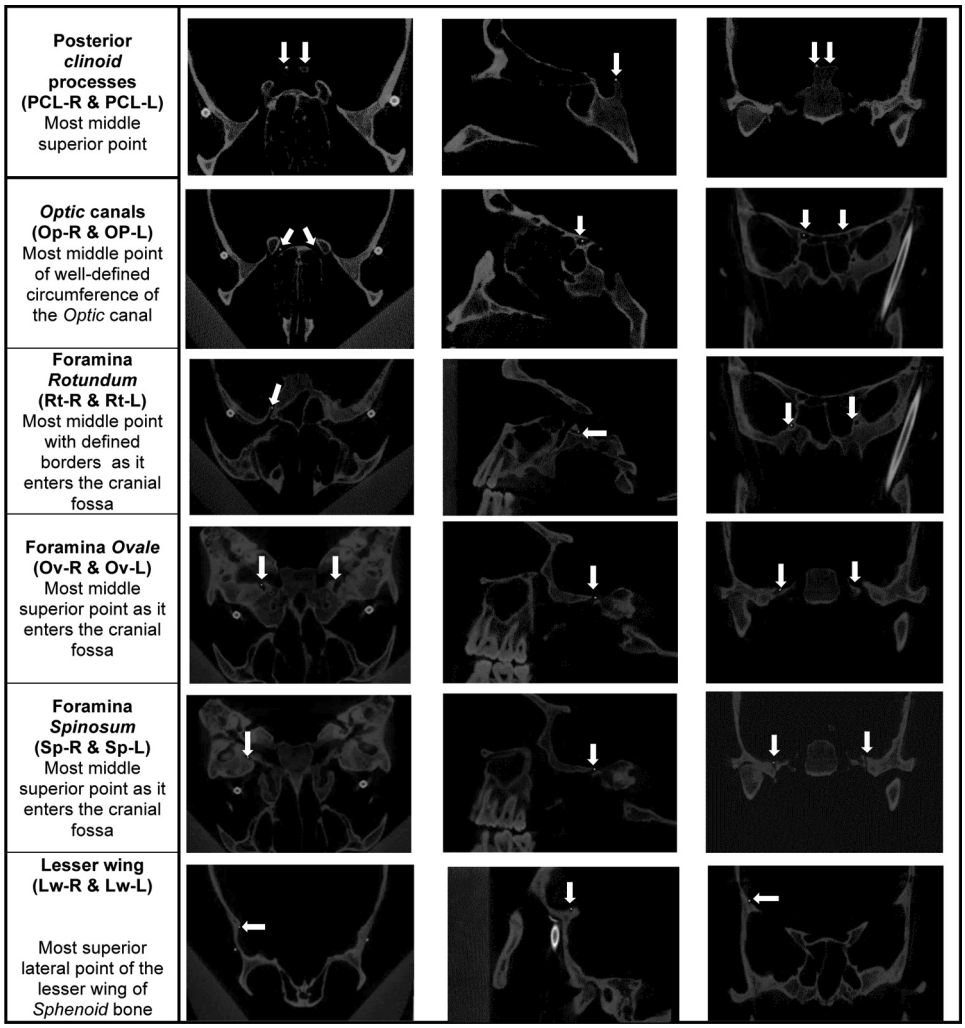

Fig. (*continued*).

We attempted to elucidate whether some preselected structures of the anterior and middle cranial bases are stable in all dimensions during a specific time period. These structures, if proven to be stable, could be used in 3D superimposition techniques.

MATERIAL AND METHODS

This investigation was a retrospective observational longitudinal study, approved by the health research ethics board at the University of Alberta in Canada (reference number Pro00043800).

To determine intrarater and interrater reliabilities and accuracy of the landmarks, 10 dry skulls were imaged with a second-generation i-CAT machine (8.9 seconds exposure time, 16 × 13-cm field of view, 0.4 voxel size) (Imaging Sciences International, Hatfield, Pa). Nineteen landmarks (Fig) were considered and located on the skulls' CBCT images using Avizo software (version 8.1; FEI Visualization Sciences Group, Mérignac Cedex, France). The images were viewed on a 14-in laptop monitor. The Avizo software allows for brightness and contrast adjustments. For intrarater reliability, this procedure was repeated 3 times for each skull with a week between trials by 1 investigator (M.A.). Coordinates were obtained for each landmark, and intrarater reliability was analyzed. To analyze the interrater reliability of landmark identification, 2 other investigators (M.L., C.F.) located the landmarks on the same 10 CBCT images of the skulls. The software creates the Cartesian origin (0,0,0) in each scan. This origin would always be the same for the same image, but it differs among different images. After we determined the reliability of the landmarks, these were marked in the dry skulls using gutta-percha. The same 10 skulls with gutta-percha

Table I. Minimum, maximum, and mean age at T1 and T2 and the difference

	n	*Minimum*	*Maximum*	*Mean*	*SD*
Age at T1 (y)	60.0	11.0	15.4	13.0	1.1
Age at T2 (y)	60.0	12.7	17.0	14.6	1.1
T2 – T1 (y)	60.0	1.2	2.0	1.6	0.2

were then reimaged, and coordinates were obtained from the gutta-percha positions. These coordinates from the gutta-percha marked landmarks were compared with the nongutta-percha marked landmarks to determine accuracy in identifying them. The reason for using dry skulls was to be able to identify reliable and accurate landmarks that can be used in the clinical data set. After we reviewed the results from the total of 19 landmarks, we eliminated 2 since they had low reliability values and were difficult to identify in the images.

To evaluate dimensional changes of the anterior and middle cranial bases with growth, CBCT images of adolescent subjects taken at 2 time points were used. The CBCT data were collected from a private practice generated from a second-generation i-CAT machine (with the same settings used for the skull data). One hundred forty-eight patients who completed orthodontic treatment between December 2008 and December 2011 were identified. Thirty-seven patients with incomplete records and 12 patients over 16 years of age at time point 1 (T1) were excluded. Therefore, a total of 99 patients had complete records with T1 and final (T2) CBCT images. From them, a final sample of 60 patients was selected. The University of Alberta orthodontic program policy does not require pretreatment and posttreatment CBCTs. The data in this study were gathered from preexisting CBCT images from a private practice. The patients had Class I and Class II malocclusions and received full fixed orthodontic treatment. Some patients had tooth-anchored expansion appliances. The assumption was that the provided orthodontic treatment did not influence the growth of the cranial base.

The inclusion criteria were the following.

1. From the 99 sets of CBCT images, 30 subjects with an age range of 11 to 13 years and 30 subjects with an age range of 13 to 15.5 years who had the longest time interval between the T1 and T2 images were selected. The interval between T1 and T2 ranged from 14 to 24 months, with most at 17 to 20 months apart (patients with CBCTs beyond that range were not included to obtain a more homogenous sample in terms of differences between initial and final CBCT images).
2. The cranial base was depicted completely in the CBCT images at both time points.

Table II. Linear measurement definitions

Anteroposterior	
1. Na-Ce	Distance between nasion and foramen caecum
2. Na-Eth	Distance between nasion and posterior border of the ethmoid bone
3. Ce-Eth	Distance between foramen caecum and the posterior border of the ethmoid bone
4. Eth-Presph	Distance between the posterior border of the ethmoid bone and posterior limit of tuberculum sella
Transverse	
1. ACL.R-ACL.L	Distance between the anterior clinoid processes right and left
2. PCL.R-PCL.L	Distance between the posterior clinoid processes right and left
3. Op.R-Op.L	Distance between the optic canals right and left
4. Rt.R-Rt.L	Distance between the foramina rotundum right and left
5. Ov.R-Ov.L	Distance between the 2 foramina ovale right and left
6. Sp.R-Sp.L	Distance between the 2 foramina spinosum right and left
Vertical	
1. Ce-Cg	Distance between foramen caecum and tip of the crista galli
2. Na-Ov.R	Distance between nasion and foramen ovale right
3. Na-Ov.L	Distance between nasion and foramen ovale left
4. Op.R-Rt.R	Distance between optic canal right and foramen rotundum right
5. Op.L-Rt.L	Distance between optic canal left and foramen rotundum left
6. Presph-Ov.R	Distance form tuberculum sella to foramen ovale right
7. Presph-Ov.L	Distance form tuberculum sella to foramen ovale left
8. MidRts-Presph	Distance between the right and left foramina rotundum to posterior limit of tuberculum sella
9. MidOvs-Presph	Distance between the right and left foramina ovale to posterior limit of tuberculum sella
10. MidSps-Presph	Distance between the right and left foramina spinosum to posterior limit of tuberculum sella

The mean age of the patients at T1 was 13 ± 1.1 years (minimum, 11 years; maximum, 15.4 years). The mean age at T2 and the mean difference between the 2 time points are given in Table I. The sample included 17 boys and 42 girls (sex of 1 patient was not recorded).

To assess anterior and middle cranial base changes due to growth, 17 landmarks (which showed good intrareliability previously) were then located on the 3D images of the patients at T1 (pretreatment) and T2 (posttreatment). Twenty linear measurements were generated (Table II) using the following equation at each time point with the Cartesian coordinates of the landmarks.

$$d = \sqrt{(x_2 - x_1)^2 + (y_2 - y_1)^2 + (z_2 - z_1)^2}$$

Table III. Intraclass correlation coefficient (ICC) values of intrarater reliability for landmarks in x, y, and z axes

	x			*y*			*z*		
Landmark	*ICC*	*ICC (lower bound)*	*ICC (upper bound)*	*ICC*	*ICC (lower bound)*	*ICC (upper bound)*	*ICC*	*ICC (lower bound)*	*ICC (upper bound)*
ACL-L	0.89	0.72	0.97	0.99	0.98	1.00	0.99	0.98	1.00
ACL-R	0.82	0.57	0.95	0.99	0.98	1.00	0.99	0.97	1.00
Ce	0.98	0.95	1.00	1.00	0.99	1.00	0.99	0.98	1.00
Cg	0.95	0.85	0.99	0.99	0.96	1.00	0.99	0.98	1.00
Eth	0.80	0.54	0.94	0.99	0.97	1.00	0.99	0.97	1.00
Na	0.90	0.73	0.97	0.99	0.98	1.00	0.99	0.96	1.00
Op-L	0.93	0.81	0.98	0.99	0.97	1.00	1.00	0.99	1.00
Op-R	0.92	0.78	0.98	0.98	0.95	1.00	1.00	0.99	1.00
Ov-L	0.82	0.57	0.95	0.93	0.82	0.98	0.99	0.98	1.00
Ov-R	0.96	0.88	0.99	0.94	0.83	0.98	1.00	0.99	1.00
PCL-L	0.91	0.73	0.98	0.98	0.95	1.00	1.00	0.99	1.00
PCL-R	0.89	0.71	0.97	0.98	0.95	1.00	1.00	0.99	1.00
PreSph	0.93	0.82	0.98	0.97	0.91	0.99	0.99	0.98	1.00
Rt-L	0.97	0.91	0.99	0.99	0.96	1.00	1.00	0.99	1.00
Rt-R	0.98	0.94	0.99	0.99	0.96	1.00	1.00	0.99	1.00
Sp-L	0.95	0.86	0.99	0.99	0.97	1.00	0.99	0.98	1.00
Sp-R	0.98	0.94	0.99	0.96	0.90	0.99	1.00	0.98	1.00
LW-L	0.55	0.16	0.84	0.90	0.73	0.97	0.93	0.82	0.98
LW-R	0.55	0.16	0.84	0.96	0.88	0.99	0.92	0.78	0.98

where d is the distance (in millimeters) between 2 anatomic landmarks, and x_1, y_1, and z_1 and x_2, y_2, and z_2 are the coordinates of the 2 landmarks at the 2 ends of the linear measurement.

Each landmark was included in multiple linear measurements of different orientations to be able to assess all dimensions (vertical, anteroposterior, transverse).

Statistical analysis

A standard statistical software package (SPSS version 20; IBM, Armonk, NY) was used for data analysis. Intrarater and interrater reliabilities were assessed using the intraclass correlation coefficient.

A sample of 60 was selected without a power analysis due to lack of a preliminary study at the time of data collection. In addition, 60 specimens are 2 times more than the number of specimens usually recommended to determine the significance in this type of study.[8] Growth changes in the cranial base were assessed by repeated-measures multivariate analysis of covariance (MANCOVA) (followed by post hoc analysis) with 1 within-subject factor of "time" with 2 levels (T1 and T2), while considering the patient's age at T1 as the covariate.

There were 20 continuous dependent variables: the distances measured in millimeters between 2 landmarks (Table II). Descriptive statistics were generated for each variable (Appendix 1). Patient age at T1 was considered as a covariate to control for differences in age of the subjects at T1.

Before we performed the repeated-measures MANCOVA statistical analysis, we checked the data for model assumptions. The overall repeated-measures MANCOVA test results suggested that age did not have a significant effect as a covariate ($F[20,39] = 1.526$; $P = 0.127$; Wilks $\Lambda = 0.561$; partial $\eta^2 = 0.439$); consequently, the covariate was eliminated, and the analysis was repeated without the covariate.

RESULTS

The majority of the selected landmarks had excellent intrarater reliability in the 3 axes of x, y, and z (Tables III and IV). Poor to moderate intrarater reliability of 2 landmarks, lesser wing right and left, and the principal investigator's (M.A.) difficulty in perceiving these landmarks radiographically were the reasons to eliminate them from the list of landmarks because they failed to be reliable 3D anatomic landmarks. Interrater reliability results are presented in Appendices 2 and 3.

The repeated-measures MANOVA test (without age at T1 as a covariate) showed evidence of a statistically significant difference between the mean of distance changes on the combined dependent variables, $F(20,40) = 6.555$; $P < 0.0001$; Wilks $\Lambda = 0.234$; partial $\eta^2 = 0.766$. The partial η^2 of the time factor (0.766) determined that time change accounted for 77% of the total variability in the linear measurements. In other words, 77% of the variability in measurements at T1 and T2 is explained by time (growth). Naturally occurring

Table IV. Intrarater absolute mean differences (mm) in coordinates of the landmarks in x, y, and z axes based on 3 readings

		x				*y*				*z*			
Landmark	*n*	*Mean*	*SD*	*Min*	*Max*	*Mean*	*SD*	*Min*	*Max*	*Mean*	*SD*	*Min*	*Max*
ACL-L	10	0.54	0.42	0	1.33	0.47	0.32	0	0.67	0.67	0.54	0	1.33
ACL-R	10	0.34	0.35	0	0.67	0.34	0.35	0	0.67	0.87	0.63	0	2
Ce	10	0.07	0.21	0	0.67	0.27	0.47	0	1.33	0.33	0.47	0	1.33
Cg	10	0.13	0.28	0	0.67	0.74	0.8	0	2.67	0.33	0.65	0	2
Eth	10	0.47	0.45	0	1.33	1	0.56	0.67	2	0.67	0.54	0	2
LW-L	10	3.13	2.11	0.67	7.33	2.27	2.44	0	6.67	1.6	1.27	0.67	4.67
LW-R	10	3.47	3.06	0	9.33	2	2.04	0	6	2.14	1.4	0.67	4.67
Na	10	0.27	0.35	0	0.67	0.33	0.65	0	2	0.4	0.35	0	0.67
Op-L	10	0.27	0.35	0	0.67	1.27	0.66	0.67	2	0.47	0.45	0	1.33
Op-R	10	0.67	0.7	0	2	1	0.96	0	2.67	0.27	0.35	0	0.67
Ov-L	10	0.53	0.53	0	1.33	1.27	0.96	0.67	3.33	0.6	0.8	0	2
Ov-R	10	0.47	0.32	0	0.67	0.8	0.98	0	3.33	0.47	0.55	0	1.33
PCL-L	8	0.5	0.47	0	1.33	0.58	0.75	0	2	0.5	0.59	0	1.33
PCL-R	10	0.87	0.55	0	2	0.67	0.54	0	1.33	0.4	0.47	0	1.33
PreSph	10	0.27	0.35	0	0.67	0.87	0.83	0	2	0.8	0.61	0	2
Rt-L	10	0.27	0.35	0	0.67	0.54	0.42	0	1.33	0.27	0.35	0	0.67
Rt-R	10	0.33	0.47	0	1.33	0.47	0.32	0	0.67	0.34	0.35	0	0.67
Sp-L	10	0.47	0.45	0	1.33	0.33	0.47	0	1.33	0.67	0.63	0	2
Sp-R	10	0.27	0.35	0	0.67	0.6	0.58	0	2	0.6	0.49	0	1.33

Min, Minimum; *Max*, maximum.

individual variability and procedural variability such as landmark positioning, measurement error, and partial volume effect could be possible sources of the remaining variability in the data. Post hoc analysis with the Bonferroni adjustment results are presented in Table V.

The pairwise comparisons showed evidence that the means of several linear measurements increased significantly from T1 to T2 (Table V).

Minor changes were found in some anteroposterior measurements. An increase of 4.9% in the distance between nasion and foramen caecum was observed, but this distance was relatively small (about 13 mm). There was suggestive but weak evidence that the distance Eth-Presph increased by 0.55 mm over time (95% confidence interval, 0.01-1.10; $P = 0.048$).

The distances measured between foramina and canals in the transverse dimension showed evidence of increases in size. However, the mean amount of increase in these transverse distances was equal to or less than 1.05 mm (from 1.1% to 4.1%). No change was observed between the right and left anterior and posterior clinoid processes.

The vertical dimension was assessed by 10 linear measurements. Among those, 5 linear measurements were from the presphenoid landmark to another true or constructed landmark in the middle cranial base. There was evidence of some changes in all 5 vertical linear measurements, but the changes were within 1.5% to 2% of the original distances.

DISCUSSION

Orthodontists are usually interested in determining whether their patients are still growing. To make that decision, some stable reference structures are needed. The serial images are superimposed on stable facial structures to determine changes in growing facial structures. Historically, the anterior cranial base sagittal dimension has been used as a reference structure in lateral cephalometry superimpositions. In this study, the growth of the skull base in the adolescent years was studied with CBCT. The anterior and middle cranial bases were assessed in the 3 dimensions of anteroposterior, transverse, and vertical during approximately 19 months.

Negligible changes were found in the anteroposterior measurements. Even though a 4.9% increase in the distance between nasion and foramen caecum was observed, this distance was relatively small (about 13 mm); therefore, measurement error does amplify and become more evident in smaller distances.[9,10] Increases in the thickness of the frontal bone, apposition in the glabella region, and size of the frontal sinus contribute to increases in the length of the anterior cranial base and forward movement of nasion until adulthood (3.3% increase in the frontal bone segment from age 6 to early adulthood, $P < 0.01$, as reported by Knott[3]).[1,4,5] These findings were similar to our results; however, in this study we

Table V. MANOVA pairwise comparisons

Distance	Mean difference T2-T1 (mm)	SD (mm)	P value	95% CI for difference		Percentage change
				Lower bound	Upper bound	
Anteroposterior						
Na-Ce	0.68	1.07	<0.0001	0.41	0.95	4.9%
Na-Eth	−0.02	1.84	0.940	−0.51	0.48	N/A
Ce-Eth	−0.34	1.93	0.182	−0.84	0.16	N/A
Eth-Presph	0.55	2.14	0.048	0.01	1.09	2.9%
Transverse						
ACL.R- ACL.L	0.18	0.98	0.173	−0.08	0.43	N/A
PCL.R - PCL.L	0.12	1.61	0.576	−0.30	0.54	N/A
Op.R-Op.L	0.98	2.05	<0.0001	0.45	1.50	4.1%
Rt.R-Rt.L	0.81	0.74	<0.0001	0.62	1.01	2.2%
Ov.R-Ov.L	0.53	1.28	0.003	0.18	0.88	1.1%
Sp.R-Sp.L	1.05	1.04	<0.0001	0.77	1.32	1.7%
Vertical						
Ce-Cg	0.12	1.17	0.399	−0.17	0.42	N/A
Na-Ov.R	0.72	1.04	<0.0001	0.43	1.00	0.9%
Na-Ov.L	0.59	1.20	<0.0001	0.29	0.90	0.8%
Op.R-Rt.R	0.02	0.94	0.826	−0.20	0.25	N/A
Op.L-Rt.L	0.05	0.87	0.633	−0.17	0.28	N/A
Presph-Ov.R	0.53	1.19	<0.0001	0.25	0.81	1.6%
Presph-Ov.L	0.50	1.36	0.007	0.14	0.86	1.5%
MidRts-Presph	0.35	0.91	0.003	0.12	0.58	2.1%
MidOvs-Presph	0.46	1.21	0.003	0.16	0.75	2.0%
MidSps-Presph	0.48	1.32	0.006	0.14	0.81	1.9%

N/A, Not applicable.

looked at a relatively short period of time (average, 19 months), and it was not expected that clinically significant changes would be observed in that time.

Since the middle part of the anterior cranial base (ethmoid bone and presphenoid region) reaches adult dimensions by about age 7 years. one should not overlook the stabilization of this area.[11,12] We could not detect any change in the position of nasion except for 1 measurement (Na-Ce) during our study period. Our findings on the anteroposterior position of nasion were contradictory: 1 measurement including this landmark (Na-Eth) did not show any change, whereas the other (Na-Ce) showed some change (the effect of the length of this segment on the findings was discussed earlier). However, nasion has been reported as an undesirable landmark to be included in measurements since its position changes with age and makes the cranial base measurements unreliable.[3,13] The anterior cranial base measurements excluding the frontal bone would possibly contribute to more accurate measurements. The foramen caecum, which is the true anterior point of the cranial base,[14] or the tip of crista galli could be possible alternatives to nasion on CBCT images.

From these results, it could be observed that the midsagittal area of the anterior cranial base from foramen caecum to the presphenoid area in the anteroposterior dimension was stable during the average 19 months of evaluation (mean age, 13 years). This finding agrees with other studies that assessed the growth of this part of the cranial base.[12]

Changes in transversal dimensions were assessed by measuring the distance between the right and left anterior and posterior clinoid processes, optic canals, and foramina rotundum, spinosum, and ovale. Interestingly, the distances between foramina and canals, measured by placing a marker of 0.25 mm at the center of the identifiable circumference of the canal or foramina (position of the identifiable circumference was different for each landmark; landmark definitions are presented in the Fig), showed evidence of an increase in size. No change was observed between the right and left anterior and posterior clinoid processes. However, the mean amount of increase in these transverse distances was equal to or less than 1.05 mm. The greatest increase was observed between optic canals right and left (4.1%, or 0.95 ± 2 mm). The examiner showed high intrarater reliability in marking all landmarks included in the study (Table III, x-axis). No contrast with previous studies was possible because changes in the transverse dimension of the cranial base have not been studied previously. Therefore, we suggest using the area between the right

and left anterior and posterior clinoid processes as stable transversal structures during the studied time period.

Finally, the vertical dimension was assessed by 10 linear measurements (Table II). Among those, 5 linear measurements were from presphenoid landmarks to another true or constructed landmark in the middle cranial base. There was evidence of some changes in all 5 vertical linear measurements, but the changes were within 1.5% to 2% of the original measurements (mean change was less than 0.53 mm). Nevertheless, Melsen[6] recognized some appositional activity in the histologic assessments of the presphenoid region in the prepubertal stages that would modify the height of the region. Björk[15] also observed apposition on the tuberculum sellae from the late juvenile years to adulthood on serial lateral radiographs. The findings of our study support their findings. One could argue that a statistically significant increase in the vertical length of the middle cranial base, even though small (≤0.53 mm, or 1.5%-2.1 %), measured from the presphenoid region was merely due to measurement error. However, the intrarater reliability of identifying the landmarks used in vertical measurements showed excellent results. It is not easy to firmly draw a conclusion whether there is a true change in a vertical dimension due to appositional activity in the presphenoid region or just the imprecision of the measurement itself. Further investigation of CBCT images taken at longer intervals would definitely help in drawing clearer conclusions.

In summary, minor changes were observed in the anterior and middle cranial base structures assessed in this study. The magnitudes of the changes were small and could reflect measurement errors. Our recommendation is to repeat the study on a different sample to confirm our findings. Isolated segments of the cranial base where the landmarks are not shared in multiple distances are suggested as preferable reference structures. Fewer variables would increase the power of the statistical analysis and reduce the cumulative effect of measurement error.

The stability of the cranial base structures was assessed during a relatively short time in this study. The CBCT images were on average 19 months apart during the adolescent years. This limitation was due to the data that were available. Ideally, a long-term observation time with more frequent CBCT images at longer intervals would give a better picture of the possible changes and help to clarify the areas of doubt with limited observation times. However, because of the health risks associated with ionizing radiation, especially in young people, obtaining frequent radiographs is not recommended.

Although statistical differences were evident between some measurements from T1 to T2, several factors affected the interpretation of the results. The voxel size of 0.4 mm could have affected the results. Since most of the mean differences in measurements from T1 to T2 were less than 1 mm (standard deviations from 0.87 to 2.14), a 0.4-mm voxel size error at both ends of a linear measurement could easily cause a magnitude of zero to 0.8 mm of difference in the distance. Therefore, the statistically significant results should be interpreted cautiously.

Measurement error should be considered in interpreting the numeric data. There are a number of sources of error influencing these data. Variations in landmark identification directly contribute to measurement error because of the cumulative nature of error.[16] In addition, in 3D images compared with 2-dimensional images, an extra dimension would be an added source of error. Also, in linear measurements, the closer the 2 landmarks constituting the segment, the greater the percentage of error introduced.[10]

Another source of measurement error in 3D radiographic imaging in this study was the possible effect of the segmentation process. The surface model construction in CBCT is based on the voxel-based data. A threshold value is specific for each structure whether it is bone or soft tissue. The threshold value and the grey value entered by the operator into the CBCT machine determine the image accuracy. Also, the CBCT imaging lacks beam homogeneity; this means that the grey values of the voxels of the CBCT images of the same subject at different time points differ.[16,17] In our study, the main method of landmark identification was multiplanar by checking the landmarks on axial, coronal, and sagittal slices. This technique would decrease the measurement error compared with relying only on surface models for location of the landmark.

There were more girls in our sample than boys (42 vs 17). We did not consider sex in our data analysis. Because girls' growth timing is different from that of boys, the results could be affected if sex had been taken into account. Nevertheless, age at T1 was not a factor as determined in the statistical analysis. This variable was considered as a proxy to indirectly determine differential adolescent peak growth timing.

CONCLUSIONS

From the dry skull analysis, 17 of the 19 landmarks preselected were deemed adequate based on their reliability and accuracy to be used in patient images.

From the CBCT images of adolescents followed for a mean of 19 months, we concluded the following.

1. The anteroposterior, transverse, and vertical dimensions of the anterior and middle cranial base structures showed relatively minor changes.
2. The midsagittal area of the anterior cranial base from foramen caecum to the presphenoid area in the anteroposterior dimension was stable.
3. The area between the right and left anterior and posterior clinoid processes appeared to be stable for transversal structures.
4. No stable structure was identified in the vertical dimension.
5. The magnitudes of the changes observed were relatively small and could reflect measurement errors.

REFERENCES

1. Ford E. Growth of the human cranial base. Am J Orthod 1958;44:498-506.
2. Steuer I. The cranial base for superimposition of lateral cephalometric radiographs. Am J Orthod 1972;61:493-500.
3. Knott VB. Change in cranial base measures of human males and females from age 6 years to early adulthood. Growth 1971;35:145-58.
4. Björk A. Cranial base development: a follow-up x-ray study of the individual variation in growth occurring between the ages of 12 and 20 years and its relation to brain case and face development. Am J Orthod 1955;41:198-225.
5. Stramrud L. External and internal cranial base a cross sectional study of growth and of association in form. Acta Odontol 1959;17:239-66.
6. Melsen B. The cranial base: the postnatal development of the cranial base studied histologically on human autopsy material. Acta Odontol Scand 1974;32(Supp 62):689-91.
7. Proffit WR, Fields HW Jr, Sarver DM. Contemporary orthodontics. 5th ed. St Louis: Elsevier Health Sciences; 2013.
8. Springate SD. The effect of sample size and bias on the reliability of estimates of error: a comparative study of Dahlberg's formula. Eur J Orthod 2012;34:158-63.
9. Nagasaka S, Fujimura T, Segoshi K. Development of a non-radiographic cephalometric system. Eur J Orthod 2003;25:77-85.
10. Baumrind S, Frantz RC. The reliability of head film measurements: 2. Conventional angular and linear measures. Am J Orthod 1971;60:505-17.
11. Scott J. The cranial base. Am J Phys Anthropol 1958;16:319-48.
12. Afrand M, Ling CP, Khosrotehrani S, Flores-Mir C, Lagravère-Vich MO. Anterior cranial-base time-related changes: a systematic review. Am J Orthod Dentofacial Orthop 2014;146:21-32.e6.
13. Pritchard JJ, Scott JH, Girgis FG. The structure and development of cranial and facial sutures. J Anat 1956;90:73-86.
14. Lieberman DE, Ross CF, Ravosa MJ. The primate cranial base: ontogeny, function, and integration. Am J Phys Anthropol 2000;(Supp 31):117-69.
15. Björk A. The use of metallic implants in the study of facial growth in children: method and application. Am J Phys Anthropol 1968;29:243-54.
16. Damstra J, Fourie Z, Huddleston Slater JJ, Ren Y. Reliability and the smallest detectable difference of measurements on 3-dimensional cone-beam computed tomography images. Am J Orthod Dentofacial Orthop 2011;140:e107-14.
17. Loubele M, Jacobs R, Maes F, Denis K, White S, Coudyzer W, et al. Image quality vs radiation dose of four cone beam computed tomography scanners. Dentomaxillofac Radiol 2008;37:309-18.

Appendix 1. Descriptive of repeated measures for all distances

		T1				T2				Difference T2-T1			
Distance	n	Mean at T1	SD	Min	Max	Mean at T2	SD	Min	Max	Mean	SD	Min	Max
1. Na_Ce	60	13.20	2.25	9.00	18.00	13.88	2.60	9.00	19.89	0.65	1.07	−2	4
2. Na_Eth	60	43.50	3.93	35.00	52.00	43.48	4.03	33.08	52.00	0.02	1.85	−4	6
3. Ce_Eth	60	32.49	4.14	21.61	41.10	32.16	4.26	21.14	39.79	0.30	1.92	−4	3
4. Eth_Presph	60	17.80	3.38	9.94	24.00	18.35	3.47	11.39	26.43	0.52	2.14	−6	6
1. ACL.R_ ACL.L	60	23.93	2.09	20.16	28.00	24.11	1.82	20.19	28.00	0.23	0.98	−1	3
2. PCL.R _ PCL.L	60	11.79	2.50	7.00	18.00	11.91	2.41	7.00	18.00	0.08	1.61	−3	4
3. Op.R_Op.L	60	22.75	2.59	17.14	32.00	23.73	2.72	19.00	31.00	0.95	2.05	−5	6
4. Rt.R_Rt.L	60	35.86	3.14	27.71	47.00	36.67	3.12	28.59	47.00	0.72	0.74	−1	2
5. Ov.R_Ov.L	60	47.94	2.71	40.90	54.00	48.47	2.93	42.40	54.00	0.42	1.28	−3	3
6. Sp.R_Sp.L	60	60.50	3.37	54.18	70.00	61.54	3.38	55.00	70.00	1.03	1.04	0	5
1. Ce_Cg	60	7.15	2.34	2.38	13.00	7.27	2.37	2.00	13.00	0.13	1.19	−2	4
2. Na_Ov.R	60	77.53	3.57	67.30	85.00	78.24	3.81	68.72	88.00	0.78	1.04	−2	4
3. Na_Ov.L	60	77.36	3.56	69.89	85.00	77.95	3.64	69.53	86.00	0.67	1.20	−3	3
4. Op.R_Rt.R	60	17.52	1.90	13.28	22.00	17.55	2.06	13.13	22.00	0.03	0.94	−3	2
5. Op.L_Rt.L	60	16.97	1.84	13.33	22.00	17.02	1.88	13.00	21.00	0.02	0.87	−2	2
6. Presph_Ov.R	60	33.48	1.88	28.71	37.00	34.00	2.31	29.02	38.00	0.48	1.19	−2	3
7. Presph_Ov.L	60	32.84	2.36	26.58	38.00	33.34	2.47	27.51	38.00	0.55	1.36	−2	3
8. MidRts_Presph	60	16.61	2.21	11.59	21.00	16.96	2.29	11.84	21.00	0.23	0.91	−2	3
9. MidOvs_Presph	60	22.88	1.92	18.63	28.00	23.33	2.12	18.00	27.25	0.48	1.21	−3	3
10. MidSps_Presph	60	25.08	1.97	21.00	31.00	25.55	2.25	21.00	32.39	0.48	1.32	−3	4

Min, Minimum; *Max*, maximum.

Appendix 2. Intraclass correlation coefficient (ICC) values of interrater reliability

	x			y			Z		
Landmark	ICC	ICC (lower bound)	ICC (upper bound)	ICC	ICC (lower bound)	ICC (upper bound)	ICC	ICC (lower bound)	ICC (upper bound)
ACL-L	0.72	0.20	0.92	0.99	0.98	1.00	1.00	0.99	1.00
ACL-R	0.61	0.08	0.88	0.99	0.96	1.00	0.99	0.98	1.00
Ce	0.95	0.86	0.99	0.99	0.97	1.00	0.96	0.87	0.99
Cg	0.90	0.69	0.97	0.98	0.94	0.99	0.98	0.94	1.00
Eth	0.70	0.33	0.91	0.72	0.32	0.92	0.96	0.87	0.99
Na	0.79	0.52	0.94	1.00	0.98	1.00	0.98	0.93	0.99
Op-L	0.80	0.48	0.94	0.98	0.94	1.00	1.00	0.99	1.00
Op-R	0.88	0.71	0.97	0.98	0.93	0.99	1.00	1.00	1.00
Ov-L	0.79	0.44	0.94	0.87	0.60	0.96	0.99	0.95	1.00
Ov-R	0.93	0.82	0.98	0.80	0.53	0.94	0.99	0.97	1.00
PCL-L	0.46	0.03	0.83	0.97	0.92	0.99	1.00	0.99	1.00
PCL-R	0.73	0.28	0.92	0.98	0.93	0.99	1.00	1.00	1.00
PreSph	0.57	0.18	0.85	0.99	0.96	1.00	0.99	0.97	1.00
Rt-L	0.55	0.15	0.85	0.96	0.90	0.99	0.96	0.90	0.99
Rt-R	0.94	0.83	0.98	0.96	0.90	0.99	0.98	0.94	0.99
Sp-L	0.78	0.50	0.93	0.79	0.53	0.94	0.99	0.97	1.00
Sp-R	0.91	0.76	0.97	0.76	0.48	0.93	0.99	0.97	1.00

Appendix 3. Interrater absolute mean differences (mm) in coordinates of the landmarks in x, y, and z axes

		x				*y*				*z*			
Landmark	*n*	*Mean*	*Min*	*Max*	*SD*	*Mean*	*Min*	*Max*	*SD*	*Mean*	*Min*	*Max*	*SD*
ACL-L	10	1.13	0.67	2.00	0.45	0.40	0.00	0.67	0.35	0.60	0.00	1.33	0.49
ACL-R	10	1.20	0.67	2.00	0.42	0.67	0.00	1.33	0.31	0.80	0.00	2.00	0.52
Ce	10	0.20	0.00	0.67	0.32	0.60	0.00	2.00	0.73	1.00	0.00	3.33	1.05
Cg	10	0.34	0.00	0.67	0.35	0.94	0.00	3.33	0.90	0.60	0.00	2.67	0.80
Eth	10	0.74	0.00	2.00	0.58	4.47	0.00	2.00	4.02	1.40	0.00	2.67	1.06
Na	10	0.60	0.00	1.33	0.38	0.40	0.00	1.33	0.47	0.60	0.00	1.33	0.49
Op-L	10	0.60	0.00	1.33	0.38	0.80	0.00	2.00	0.52	0.34	0.00	0.67	0.35
Op-R	10	0.80	0.00	1.33	0.42	0.87	0.00	2.00	0.63	0.07	0.00	0.67	0.21
Ov-L	10	0.87	0.00	1.33	0.45	1.93	0.00	6.67	1.85	1.13	0.00	2.00	0.55
Ov-R	10	0.54	0.00	1.33	0.42	1.67	0.00	8.00	2.29	0.93	0.00	2.00	0.72
PCL-L	8	1.17	0.00	2.67	0.93	1.08	0.00	2.00	0.61	0.50	0.00	1.33	0.47
PCL-R	10	1.33	0.00	3.33	1.04	0.87	0.00	2.00	0.63	0.20	0.00	0.67	0.32
PreSph	10	0.93	0.00	2.67	0.84	0.47	0.00	2.00	0.63	0.80	0.00	1.33	0.42
Rt-L	10	1.13	0.00	4.67	1.41	1.07	0.00	2.00	0.64	1.20	0.00	4.67	1.29
Rt-R	10	0.60	0.00	1.33	0.66	0.93	0.00	2.00	0.56	0.87	0.00	4.00	1.18
Sp-L	10	0.87	0.00	2.67	0.83	1.20	0.00	9.33	2.89	1.07	0.00	2.00	0.64
Sp-R	10	0.60	0.00	2.00	0.58	1.07	0.00	8.67	2.69	1.07	0.00	2.00	0.72

Min, Minimum; *Max*, maximum.